Mon. Not. R. Astron. Soc. 296, 824–838 (1998)

Spectroscopic survey of field Type II Cepheids

József Vinkó,[1,2] Nancy Remage Evans,[3,4] László L. Kiss[5] and László Szabados[6]

[1]*Research Group on Laser Physics of the Hungarian Academy of Sciences and Department of Optics, JATE University, Szeged, Dóm tér 9, H-6720 Hungary*
[2]*Hungarian Eötvös Fellowship, Department of Physics and Astronomy, York University, 4700 Keele Street, Toronto, Canada*
[3]*Smithsonian Astrophysical Observatory, Cambridge, Massachusetts, USA*
[4]*Department of Physics and Astronomy, York University, Toronto, Canada*
[5]*Department of Experimental Physics, JATE University, Szeged, Hungary*
[6]*Konkoly Observatory, Budapest, PO Box 67, H-1525 Hungary*

Accepted 1997 December 10. Received 1997 October 13; in original form 1997 May 20

ABSTRACT

A sample of relatively bright, short- and intermediate-period ($P = 1$–10 d) Type II Cepheids in the Galactic field have been observed spectroscopically with an intermediate-resolution ($\lambda/\Delta\lambda = 11\,000$) spectrograph. The wavelength region was 6500–6700 Å, including the Hα line and some photospheric iron lines. The signal-to-noise ratio (S/N) was usually between 50 and 100, depending on weather conditions and the brightness of target stars. Radial velocities were determined by cross-correlating the Cepheid spectra with those of selected IAU velocity standard stars having F–G spectral types. The internal error of the velocity determination process was calculated to be about 1 km s^{-1}. Hα emission and strong line splitting were observed in BL Her during the expansion phase, but no similar phenomenon was detected in any other stars in this programme, except for AU Peg which has an unusual Hα line showing a P Cygni-like profile. The velocity curve agrees well with recent CORAVEL measurements. The velocity gradients in Cepheid atmospheres are studied using the Hα minus metallic velocities. Similar data are collected from the literature. It seems that having large velocity differences ($v_{\mathrm{H}\alpha} - v_{\mathrm{metal}} > 40$ km s^{-1}) is a characteristic feature of the very short-period ($P < 1.5$ d) and longer period ($P > 10$ d) Cepheids. Between these period regions the Cepheid atmospheres exhibit smaller velocity differences. Most of the Type II Cepheids observed in the present study fall into this latter category. There might be a tendency for classical Cepheids of intermediate period to have larger maximum velocity differences.

Key words: stars: atmospheres – stars: oscillations – Cepheids.

1 INTRODUCTION

Cepheid-type variable stars play a major role in both Galactic and extragalactic distance measurements, which can be exemplified by the recent Hubble Key Project aimed at measuring the Hubble constant. Due to their primary importance, it is essential to know and understand the basic physical properties as well as the details of pulsational processes of Cepheids.

It has been well known for decades that Cepheids can be divided into at least two major groups: (i) the Type I (classical) Cepheid group containing massive, Population I supergiant pulsators, and (ii) the less luminous, much more heterogeneous Type II Cepheid group. Detailed reviews of Type II Cepheids have been given by Wallerstein & Cox (1984) and Gingold (1985).

Like other physical properties, the spectral characteristics of Type II Cepheids are also different from those of Type I, as has been pointed out in many papers (e.g. Kraft, Camp & Hughes 1959; Wallerstein & Cox 1984; Wallerstein & Elgar 1992). In the spectra of longer period ($P > 10$ d) stars such as the prototype W Vir, strong H and He emission is present during rising light (Joy 1949; Sanford 1952; Abt 1954; Harris & Wallerstein 1984; Raga, Wallerstein & Oke 1989; Lèbre & Gillet 1992); this emission is absent or very weak in classical Cepheid spectra (Sasselov & Lester 1990; Wallerstein et al. 1992; Breitfellner & Gillet 1993). The phases of emission of the spectra of long-period Population II Ceph-

eids are, in fact, very similar to those of other long-period variables, namely RV Tauri or Mira stars (Kraft et al. 1959; Baird 1982; Hinkle, Hall & Ridgway 1982; Pollard et al. 1997).

Such emission has not been found in Type II Cepheids of intermediate period ($3 < P < 10$ d; Harris & Wallerstein 1984), while BL Her, the prototype of short-period ($1 < P < 3$ d) Type II Cepheids, show weak Hα emission during expansion that moves across the line profile from the blue side to the red, similar to RR Lyrae stars (Gillet et al. 1994). In addition, some Type I and II Cepheids exhibit strong line doubling and changing line asymmetry at certain phases close to velocity maximum (for details, see the references given above). These spectral features were globally explained as effects of shock waves moving through the pulsating atmosphere (Schwarzschild 1952; Fokin & Gillet 1994).

It is puzzling why the atmospheres of Type II Cepheids seem to be much more affected by shocks than those of classical Cepheids, although there are a few suggestions in the literature about this question. Wallerstein & Cox (1984) suspect higher He/H ratio for W Vir itself (because both He and H lines can be seen in emission in the spectrum of W Vir), which would result in a lower sound speed and lower threshold for shocks to occur. The problem with this interpretation is that He emission cannot be seen in other Population II Cepheids except W Vir, according to Wallerstein & Cox. Wallerstein & Elgar (1992) suggest lower density gradients in the outer atmospheres of Type II Cepheids due to the much lower mass of these stars, which may also facilitate shock forming. On the other hand, the photospheric gravities of both types of stars are about the same. Moreover, there are probably strong velocity gradients in both types of atmospheres, as indicated by the large differences between the velocities of Hα and photospheric lines (Wallerstein et al. 1992), or between velocities derived from lines in the optical and infrared spectrum (Sasselov & Lester 1990).

The main aim of this paper is to contribute to the observational basis of the solution of the problem of Type II Cepheid atmospheres. Due to the faintness of these variables, spectroscopic observations with sufficient wavelength and time resolution have been available for only a few stars (mostly BL Her, κ Pav and W Vir). The initial idea was to investigate the problem of presence/absence of Hα emission in the $3 < P < 10$ d period interval by extending the number of available observations. If the behaviour were the same as for long-period Cepheids (strong emission in Type II, no emission in Type I stars) this would be a very useful method to distinguish between Type I and Type II Cepheids independently of their metal content and kinematics.

Modern spectroscopic data of Type II Cepheids are not very numerous. So far, the most extensive homogeneous survey was performed by Harris & Wallerstein (1984), who reported the lack of emission in the short-period regime, as in earlier studies (Wallerstein 1958; Kraft et al. 1959). More recently, Wallerstein et al. (1992) published a comparative analysis of Hα and metallic velocities and velocity differences for a sample of bright classical Cepheids, including κ Pav as a Type II star. Because the emission features and large velocity gradients may have a common origin, we also tried to investigate the Hα minus photospheric velocity differences for some bright northern Type II Cepheids similarly to Wallerstein et al., although the phase coverage is less complete than that of the data analysed by them. In what follows the observations and data reduction are presented, and then the results are discussed.

2 OBSERVATIONS

The stars observed for this project are listed in Table 1. The observing programme was carried out at David Dunlap Observatory with the Cassegrain spectrograph attached to the 74-in telescope. The detector was a Thomson 1024×1024 CCD chip (with a 6 e^- readout noise), and the dispersion was 10.5 Å mm^{-1} giving a resolution $\lambda/\Delta\lambda \approx 11\,000$ at Hα. The 200-Å-wide spectra were centred on 6600 Å. This spectral region contains the Hα line, several photospheric metal (mostly Fe I) lines and a considerable set of telluric lines at the blue side of Hα. The exposure times were chosen between 10 and 40 min, depending on target brightness, in order to reach S/N $\geq$ 50. Longer exposures would have been heavily affected by cosmic rays, and, since this programme was designed as a survey and was not intended to reach very high S/N ratios, the maximum exposure time was restricted to 40 min.

The spectra were reduced with standard IRAF routines, including bias removal, flat-fielding, cosmic ray elimination and wavelength calibration. For wavelength calibration, two FeAr spectral lamp exposures (obtained immediately before and after every stellar exposure) were used. For telluric line identification, at least one telluric standard star was observed each night. Since telluric lines affected only the blue side of our spectra and the S/N ratio did not allow us to obtain high-precision line profiles, the telluric lines were not removed, but the affected region was omitted from the further analysis. The spectra were normalized to the continuum by fitting cubic splines to the regions outside the Hα and telluric regimes. Again, due to the lower S/N ratios, equivalent width measurements of weak lines could not be done with sufficient accuracy; thus performing a more precise continuum normalization was not essential.

Table 1. The list of programme stars with their photometric epochs and period as well as spectral type. The data are based on the values given in the General Catalogue of Variable Stars (GCVS), but the photometric ones have been updated using recently obtained light curves.

Star	Epoch	Period (d)	Sp
BL Her	46200.316	1.30744	F0-F6
SW Tau	41687.456	1.58358	A7
AU Peg	50004.5	2.412	F8
DQ And	41998.140	3.20056	K-M
BD Cas	41935.547	3.65090	?
V572 Aql	42694.273	3.76809	?
V383 Cyg	47412.822	4.61227	?
KL Aql	47760.858	6.10801	F6-G6
TX Del	42947.033	6.16591	F8
V733 Aql	48874.815	6.17875	F9
BB Her	46620.994	7.50794	G5
IX Cas	47348.390	9.15455	F7
AP Her	49902	10.4	F2-G0

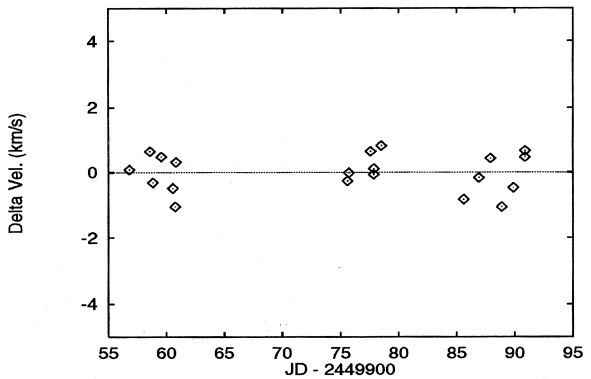

Figure 1. Differences of velocities of IAU standard velocity stars with respect to HD 222368. The scattering represents the overall error caused by the reduction procedure. The rms scatter is about 0.6 km s^{-1}, and the maximum difference is 1 km s^{-1}. This latter value is the usual uncertainty of the velocities obtained by cross-correlation technique.

Having a set of wavelength-calibrated, continuum-normalized spectra, radial velocities were determined by cross-correlating the Cepheid spectra with those of selected IAU standard velocity stars of F–G spectral types using the IRAF task *fxcor*. The barycentric corrections (due to the motion of the Earth) were calculated with the *rvcorrect* task. At first, the accuracy of the velocity system was tested by processing the standard velocity star spectra with HD 222368 as an overall template star. Fig. 1 shows the results where, in the ideal case, all velocities should be exactly zero. So the scatter in this diagram represents the overall error of the spectral reduction, the cross-correlation and the barycentric correction. The standard deviation of the data shown is $\sigma = 0.56$. We expect that the true error should be slightly increased by the lower S/N of Cepheid spectra (because the standard velocity stars were usually much brighter); thus the final error of the velocities is estimated to be 1–2 km s^{-1}. There is a possibility that night-to-night variations in the standard star spectra may also contribute to the scattering in Fig. 1, but even if this is so, it is within the estimated uncertainty of our velocity measurements.

The estimate measurement accuracy can be justified comparing our data with other velocity curves taken from recent literature. Unfortunately, such comparison is restricted to a few stars due to the lack of high-quality spectral data of Type II Cepheids. In Fig. 2 the velocities of four programme stars are plotted against phase, together with the recent CORAVEL data by Gillet et al. (1994) for BL Her and by Gorynya et al. (1996) for the other stars. It can be seen that the overall agreement is quite good; minor discrepancies, however, can be seen around the velocity maximum and at the resonance bump of BL Her. At these phases the spectral line profiles are expected to be the most asymmetric and quickly variable, so the disagreement may be due to these complexities. It is also possible that these discrepancies are real and due to cycle-to-cycle changes in the shape of the velocity curve, but there are not enough homogeneous observational data available to prove or reject this hypothesis. Note that Evans & Lyons (1986) found similar disagreement when comparing velocity curves measured with different techniques by several authors. Because these differences can affect the amplitude as well as the γ-velocity of the measured velocity curves considerably, this problem needs further attention.

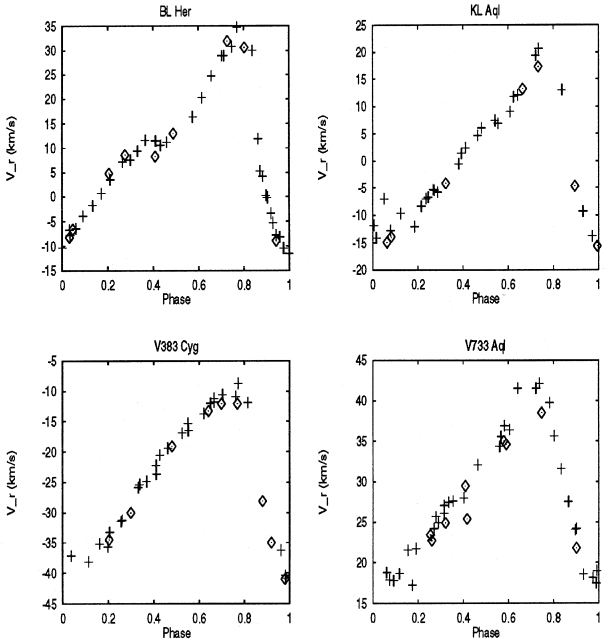

Figure 2. Comparison of the velocities of some of the programme stars measured by us (diamonds) and others (crosses) which were also determined with correlation (CORAVEL) technique (see text for references). The agreement is acceptable in most phases except around the velocity maximum and the resonance bump.

Recenty, Butler (1993) and Sabbey et al. (1995) discussed and compared various techniques to obtain radial velocity curves for Cepheids. It was shown that the technique that would satisfy all requirements is not at our disposal. This is mainly due to the variations of the line profile (changing asymmetry, broadening, sometimes emission) which are difficult to be taken into account. Many authors (e.g. Wallerstein et al. 1992) prefer the line bisector technique, choosing the bisector level at various depths. We believe that in the case of lower spectral resolution the cross-correlation technique may be better for weak lines than measuring line centres and bisectors of a few individual lines. This might be strengthened by the fact that, in contrast with the classical Cepheids measured by the authors mentioned above, most of our programme stars seemed to show less asymmetric and less complicated line profiles (especially Hα; see below). This is probably due to their shorter period and smaller velocity amplitude.

For cross-correlation velocities the crucial point is the spectral type of the template (standard velocity) star. Choosing the best template is not obvious because Cepheids can change their spectral type considerably during pulsation, and the template spectrum should match the Cepheid spectrum as closely as possible along the whole pulsational cycle. Constancy of the spectral type of the template may introduce a phase-dependent error in the cross-correlation velocities. The amount of this error, however, is probably small, because the cross-correlation integral is much more sensitive to wavelength shifts than variations in the relative intensities of spectral lines.

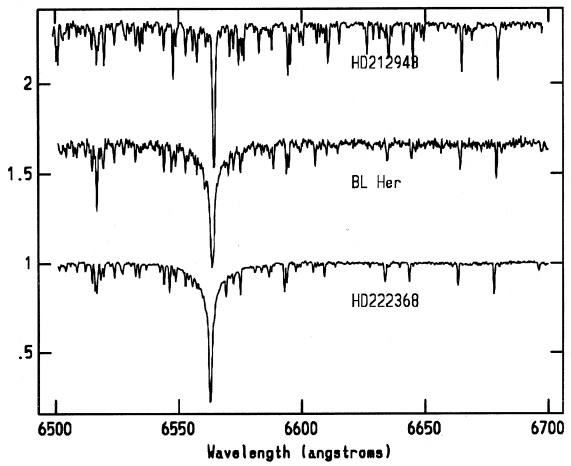

Figure 3. Comparison of spectra of BL Her and two standard velocity stars. Relative intensities normalized to the continuum are plotted against wavelength. An arbitrary vertical shift was added to each spectrum for better visibility.

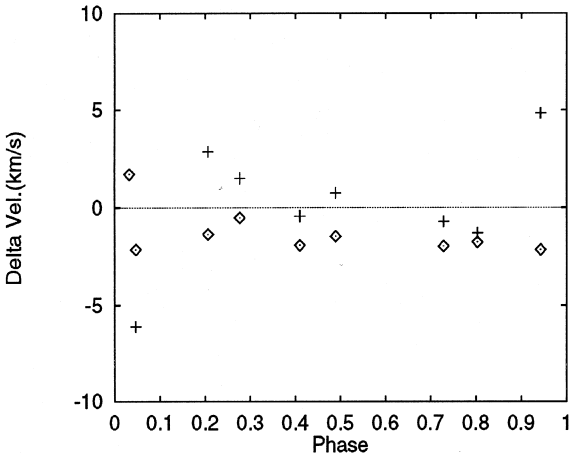

Figure 4. Differences of the metallic-line velocities (diamonds) and Hα velocities (crosses) of BL Her computed with the two different templates shown in Fig. 3 as a function of pulsational phase.

Another problem concerning template selection may be caused by the different metal content of Type II Cepheids and the template stars, because the former may have significantly lower metal abundance. This problem did not occur in the case of the programme stars of this paper, because they belong to the 'metal-rich' Type II Cepheids, so they have solar-like metallicities (except SW Tau).

To test the accuracy of the velocity determination method further, we compared the velocities of BL Her computed using two different templates. The first template (HD 222368, Sp = F7) was chosen to match the spectral type of BL Her as closely as possible (F0–F6), while the other one (HD 212943) was selected as an obviously inadequate template having K0 spectral type. Fig. 3 shows the two template spectra and one BL Her spectrum for comparison. Nine spectra of BL Her were cross-correlated with the two template spectra, and the heliocentric pulsational velocities were determined. The correlation was restricted to the 6600–6700 Å wavelength interval, so the resulting velocities correspond to the average Doppler shifts of the metallic lines in this interval. All velocities were corrected for the heliocentric velocity of the template and the motion of the Earth, as mentioned above.

The difference between these two data sets is plotted against the pulsational phase of BL Her in Fig. 4. It is apparent that for the metallic lines most of the differences are between 1 and 2 km s^{-1} ($\sigma = 1.23$), which is about the error of the derived velocities, but these differences seem to be systematic at most phases (the average value is -1.6 km s^{-1}). This systematic difference is probably due to uncertainty of the zero-point of the wavelength calibration, as the direct cross-correlation between the spectra of standard stars indicate (see Fig. 1). The situation is similar for the hydrogen line having slightly larger deviations (about 5–6 km s^{-1}) at some phases. The Hα velocities were computed with the same cross-correlation procedure, except that the selected wavelength interval was between 6550 and 6580 Å. Note that the Hα velocity difference corresponding to the earliest phase (0.03) is not plotted, because it deviates more than 60 km s^{-1} from all the other data due to the strong splitting of the hydrogen line in this phase. The larger differences of the hydrogen velocities derived from the two different templates are probably due to the sensitivity of the Hα line profile to the spectral type. Moreover, some weak metallic lines close to Hα that were included in the cross-correlation may alter the Hα velocities slightly, but this effect is probably small, because of the much stronger hydrogen line. The fact that the Hα and metallic-line velocities agree within a few km s^{-1} indicates that the change of the spectral type of the Cepheid is not a serious problem for computing metallic-line velocities by cross-correlation. Thus we conclude that for metallic lines the error caused by the mismatch of the spectral type of the Cepheid and the template is probably under the 1–2 km s^{-1} limit, i.e., it is within the uncertainty of the whole procedure. From Fig. 4 we also estimate that the error of Hα velocities probably does not exceed 4–5 km s^{-1}. Note that BL Her exhibits the largest variations of its Hα profile among our programme stars, so the uncertainties of the velocities caused by this effect are expected to be smaller for all the other Cepheids in this paper.

At the urging of the referee, we have plotted the same diagram as in Fig. 4 for all the other programme stars to verify that there are indeed no deviations in the velocity differences exceeding the limits mentioned above. The difference between metallic-line velocities was always less than 2 km s^{-1}, indicating that the errors of our absolute velocities are probably not more than this value. Systematic offsets of about 1 km s^{-1}, similar to the case of BL Her, were present in some cases, which can again be explained by the zero-point uncertainties of the wavelength calibration. The hydrogen velocities also did not show any differences larger than 5 km s^{-1}. The referee also suggested the possibility of the phase dependence of the velocity differences of the Hα line. This is indeed a possibility, and it may be due to the higher sensitivity of the sharp-lined, late spectral type template star (HD 212943) to the phase-dependent asymmetries of the Hα line of the Cepheid. However, since the Hα

cross-correlation velocities are difficult to assign to 'real' atmospheric velocities (see the discussion below), we have not studied this effect in more detail except to ensure that the errors of our Hα velocities are below the ± 5 km s^{-1} limit.

Investigating the uncertainties of the Hα velocities due to the measurement technique, we also computed bisector velocities for the Hα line selecting the 0.5, 0.7 and 0.9 bisector levels. Fig. 5 contains the plot of these velocities as a function of phase for BL Her and KL Aql. The general trend of these velocities is very similar to those presented by Wallerstein et al. (1992) using the 0.9 and 0.5 bisector levels; namely, the largest differences occur at the outward acceleration phase (roughly between 0.8–1.0), the 0.5 bisector velocities being much lower than the 0.9 bisector velocities at these phases. For BL Her the cross-correlation velocities represent roughly the 0.5 bisector velocities at most phases, except at the piston phase when these are much closer to the 0.7 bisector velocities. For KL Aql the agreement between the various types of velocities is much better, the only exception being that the cross-correlation velocities are less positive around the velocity maximum than the bisector velocities. The better agreement is probably due to the less complicated Hα profile of KL Aql (see Section 3). Unfortunately, the phase coverage of our data is not enough to discuss this problem in more detail, except to note that it seems that for strong lines the cross-correlation velocities cannot be assigned to a specific portion of the line profile. Moreover, the Hα line forms over different depths in the atmosphere, and so the physical meaning of these velocities is less clear than those of metallic lines.

Concerning the velocities of metallic lines, the resolution of our Cassegrain spectra was not high enough to derive reasonable bisector velocities. The comparison of bisector and cross-correlation velocities was therefore made using the high-resolution echelle spectra of classical Cepheids obtained by L. Kiss also at the DDO in 1996 (Kiss et al., in preparation). It turned out that the differences between the two types of velocities are below 1 km s^{-1} during the whole pulsational cycle, which means that the cross-correlation velocities of our lower resolution spectra are probably in good agreement with the bisector velocities of the same lines. The mixing of various types of velocities can therefore be allowed for metallic lines (with an accuracy of ~ 1 km s^{-1}), but not for Hα.

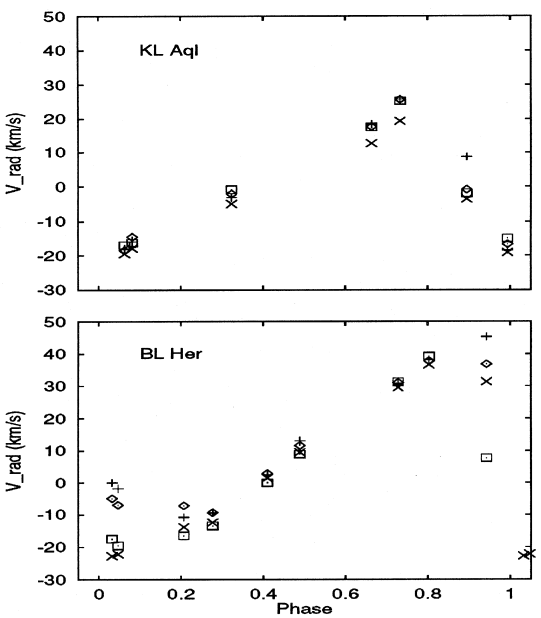

Figure 5. Comparison of Hα cross-correlation velocities (crosses) with those derived from bisectors at 0.5 (squares), 0.7 (diamonds) and 0.9 (plus signs) levels. The agreement is much better in the case of KL Aql due to its less complicated Hα profile.

3 RESULTS AND DISCUSSION

For each star listed in Table 1 the cross-correlation velocities are collected in Table 2. Figs 6–18 contain the cross-correlation velocity curves derived from metallic lines (diamonds) and the Hα line (crosses) plotted against phase (the epochs and period values can be found in Table 1). The plots have been ordered by period, although the discussion below often groups them by physical characteristics. Note that the plotted velocities of TX Del and IX Cas have been corrected for binary motion using the orbital elements derived by Harris & Welch (1989). An attempt was made to do the same for AU Peg using the orbital elements given by Harris, Olszewski & Wallerstein (1984). However, that orbit turned out to be inaccurate for this purpose. This is probably due to the strong and unpredictable pulsation period variation of AU Peg which must be monitored by photometry in order to construct a relevant pulsational velocity curve. We were continuously following the light variation of AU Peg over the past few years, including the interval of the present spectroscopic observations, and we derived a pulsational period of $P_{\rm pul} = 2.412$ d with reasonable accuracy. This enabled us to separate the pulsational and orbital velocities via Fourier analysis ($P_{\rm orb} = 53.3$ d was adopted from Harris et al. 1984), which are listed in Table 3 together with those of TX Del and IX Cas. Details of the analysis of the AU Peg velocities will be given in a subsequent publication (Vinkó et al., in preparation).

The upper panels of Figs 6–18 also show the observed spectra on the 6520–6600 Å wavelength regime (including Hα). In what follows, a short discussion of the individual variables is given.

BL Her

This star, the prototype of its class, has been observed recently by Gillet et al. (1994) with high resolution. Our observations fully confirm the conclusions of that paper – strong Hα doubling at the velocity minimum and the appearance of a weak emission feature before that (the latter is less markedly present in our spectra due to their inadequate phase coverage). All of these were successfully modelled recently by Fokin & Gillet (1994) as the effect of shock waves. This phenomenon appears to be analogous to that observed commonly in long-period Type II Cepheids and partly confirms the prediction, made by Kraft et al. (1959), that short-period Type II Cepheids can show hydrogen emission on very short time-scales.

SW Tau

This is the other well-known BL Her-type star in our programme, with a period less than 2 d. Unfortunately, the phase coverage is worse than in the case of BL Her, and the

Table 2. Cross-correlation velocities of programme stars.

JD	phase	V_{metal}	$V_{H\alpha}$	JD	phase	V_{metal}	$V_{H\alpha}$
BL Her	Template: HD222368 (F7V)						
49955.561	0.2066	4.8	−13.8	49960.582	0.0469	−6.6	−22.2
49957.551	0.7286	31.9	29.5	49961.571	0.8033	30.6	36.6
49958.546	0.4896	13.0	9.5	49988.513	0.4100	8.3	1.5
49959.575	0.2767	8.6	−12.4	49990.517	0.9427	−8.9	31.3
49960.563	0.0324	−8.2	−22.8				
SW Tau	Template: HD187691 (F8V)						
49987.890	0.5495	12.0	10.2	49991.902	0.0830	−5.8	−10.5
49988.883	0.1766	−2.8	−8.7	50007.773	0.1052	−6.4	−12.2
49989.899	0.8182	25.1	33.1	50009.726	0.3385	2.7	4.9
49990.888	0.4427	4.3	7.3				
DQ And	Template: HD212943 (K0III–IV)						
49959.834	0.5953	−221.2	−220.3	49989.766	0.9474	−232.5	−219.4
49978.730	0.4992	−227.7	−226.8	49990.833	0.2808	−241.8	−246.8
49987.855	0.3503	−237.2	−244.7	49991.823	0.5901	−222.7	−219.0
49988.838	0.6574	−220.3	−218.8				
BD Cas	Template: HD23169 (G2V)						
49959.868	0.8649	−54.5	−56.5	49988.808	0.7917	−52.1	−54.4
49961.897	0.4207	−41.1	−42.6	49989.855	0.0785	−54.6	−57.8
49978.656	0.0111	−53.7	−56.8	49990.831	0.3459	−43.8	−45.9
49979.894	0.3502	−43.1	−42.9	49991.793	0.6094	−40.9	−40.5
49987.789	0.5126	−39.6	−39.6				
V572 Aql	Template: HD187691 (F8V)						
49958.651	0.8673	44.7	39.6	49988.625	0.8220	45.1	44.4
49961.686	0.6727	58.5	57.7	49989.607	0.0826	41.4	38.7
49976.649	0.6437	61.5	60.6	49990.599	0.3459	51.4	47.8
V383 Cyg	Template: HD136202 (F8IV–V)						
49957.731	0.7697	−12.1	−4.6	49978.622	0.2991	−30.0	−27.7
49958.701	0.9800	−41.0	−42.1	49988.685	0.4809	−19.1	−15.6
49959.733	0.2037	−34.5	−35.6	49989.691	0.6990	−12.1	−4.8
49961.753	0.6417	−13.3	−7.2	49990.709	0.9197	−35.0	−30.9
49976.690	0.8802	−28.1	−16.9				
KL Aql	Template: HD204867 (G0Ib)						
49957.693	0.6644	13.2	12.7	49988.656	0.7336	17.3	19.3
49959.706	0.9939	−15.6	−19.1	49989.642	0.8950	−4.7	−3.5
49961.721	0.3238	−4.17	−4.9	49990.668	0.0630	−14.9	−19.5
49978.566	0.0817	−13.9	−17.9				
V733 Aql	Template: HD204867 (G0Ib)						
49957.669	0.2546	23.4	20.1	49976.620	0.3217	24.9	22.9
49958.626	0.4095	29.5	27.0	49988.602	0.2610	22.7	20.6
49959.681	0.5802	35.0	33.6	49989.568	0.4173	25.4	25.6
49960.717	0.7479	38.5	44.5	49990.641	0.5910	34.6	35.5
49961.667	0.9017	21.8	22.4				
BB Her	Template: HD145001 (G5III)						
49957.593	0.4136	88.1	86.1	49960.605	0.8148	103.6	113.8
49958.572	0.5440	96.3	89.1	49961.601	0.9474	78.8	76.4
49959.615	0.6829	106.8	104.2	49988.546	0.5363	93.6	88.5
AP Her	Template: HD222368 (F7V)						
49957.631	0.3491	−29.7	−36.8	49976.575	0.1707	−35.7	−28.1
49959.646	0.5429	−21.3	−31.7	49978.532	0.3588	−26.9	−28.2
49960.660	0.6404	−15.3	−26.4	49988.573	0.3243	−29.8	−27.4
49961.628	0.7335	−14.5	−17.4	49990.563	0.5157	−23.1	−27.5

phase of velocity reversal is sampled quite poorly. Nevertheless, the behaviour of Hα seems to be less complicated than that of BL Her, and the velocity differences between metallic and hydrogen lines also appear to be smaller. This might be reasonable, because the light curves of SW Tau and BL Her are different. In addition, the metal content of SW Tau is significantly lower than that of BL Her. For these reasons, different atmospheric behaviour is not unexpected. Note, however, that the poor phase coverage at velocity reversal prevents us from drawing a more reliable conclusion.

AU Peg

The classification of this peculiar Cepheid is uncertain. It is usually placed among the Type IIs because of its complex

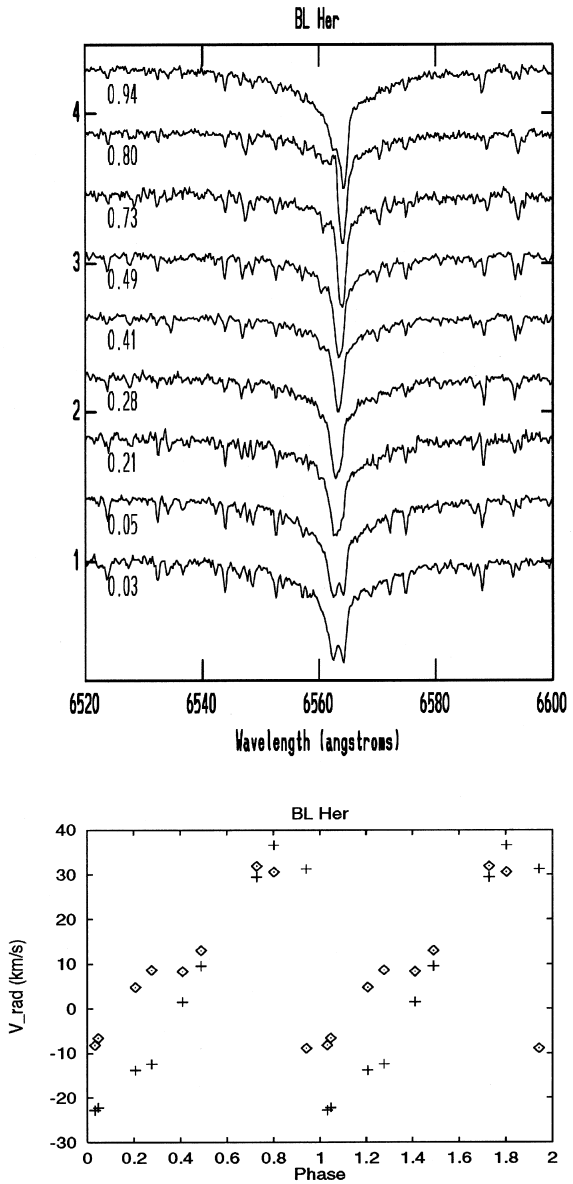

Figure 6. Hα line profiles and velocities of BL Her. The spectra were normalized to the continuum and shifted vertically. In the upper panel the relative intensities are indicated on the vertical axis. Each spectrum is labelled with the pulsational phase. In the lower panel both the metallic velocities (diamonds) and Hα velocities (crosses) determined by cross-correlation are plotted against phase.

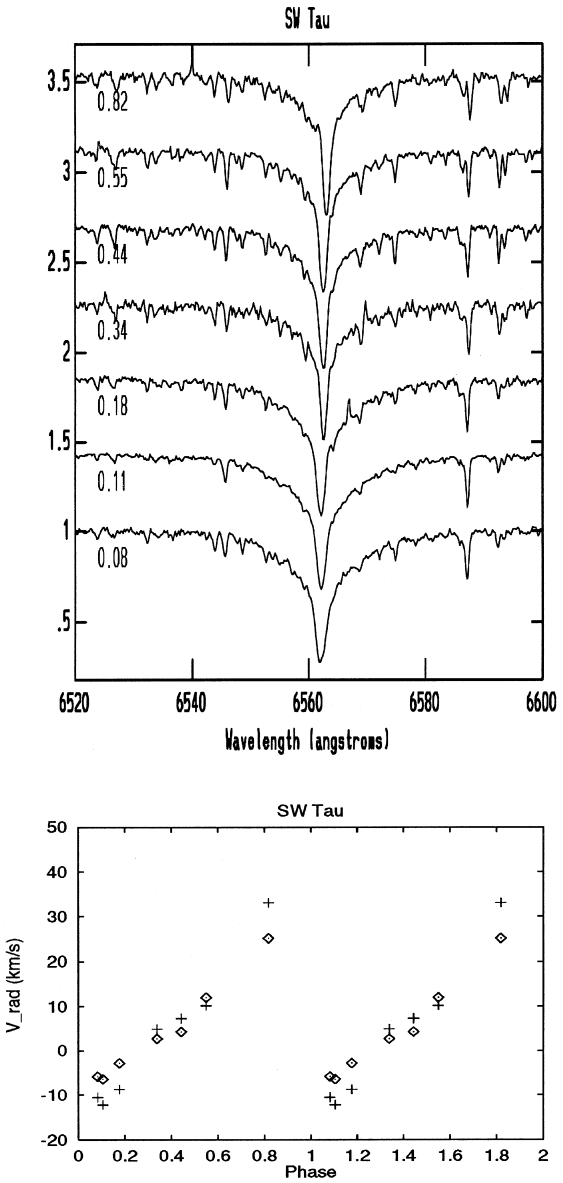

Figure 7. The same as Fig. 6 for SW Tau.

characteristics. AU Peg belongs to a binary system with the shortest orbital period among Cepheids, and it also shows strong pulsational period increase (e.g. Vinkó, Szabados & Szatmáry 1993). The Hα profiles are very different from those of any other Cepheids in this programme. There is a narrow emission feature on the red side of Hα, which does not vary during one pulsational cycle. Due to this peculiar nature, AU Peg was followed over a longer period (about 50 d, covering the whole orbit), and it was discovered that the emission feature does show variations on the orbital time-scale. About 20 spectra were colleced during this observing run (and only five of them are plotted in Fig. 8), and these will be published elsewhere together with the analysis of the velocities mentioned above. Here we only briefly note that this particular Hα profile might be due to an interaction between the circumstellar matter around AU Peg (which is quite dense according to the results of McAlary & Welch 1986) and the outer atmosphere of the star.

TX Del, IX Cas

These stars are also binaries, and so their velocities should be corrected for orbital motion (see above). No effects of the companion stars can be seen in either spectrum, except for the Doppler shift due to orbital revolution. This is a usual situation for other binary Population I Cepheids whose companions are probably main-sequence stars or slightly evolved; the luminosity of the companion is therefore much smaller than that of the Cepheid component (Evans 1991, 1992). Moreover, according to recent Baade–Wesselink solutions (Laney 1995; Balog, Vinkó & Kaszás

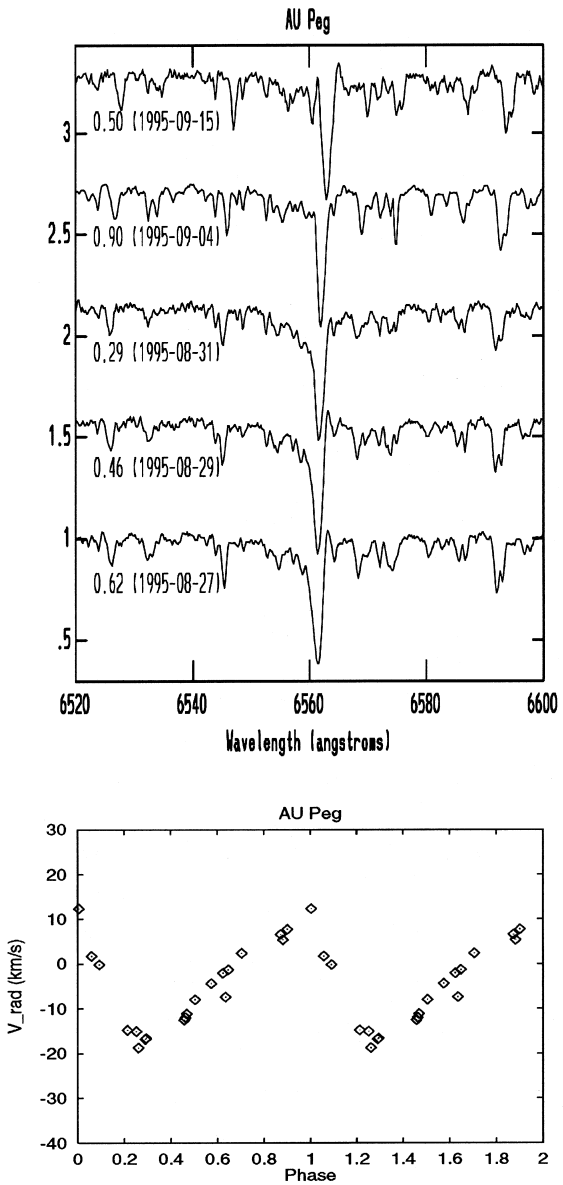

Figure 8. The same as Fig. 6 for AU Peg. The Hα velocities are substantially affected by the varying emission feature, and so they are omitted in the velocity plot (lower panel). The velocities have been corrected for the orbital motion (see text). Only five line profiles are plotted to illustrate the unusual shape and behaviour of Hα. The spectra are labelled with both the pulsational phase and the date of the observation.

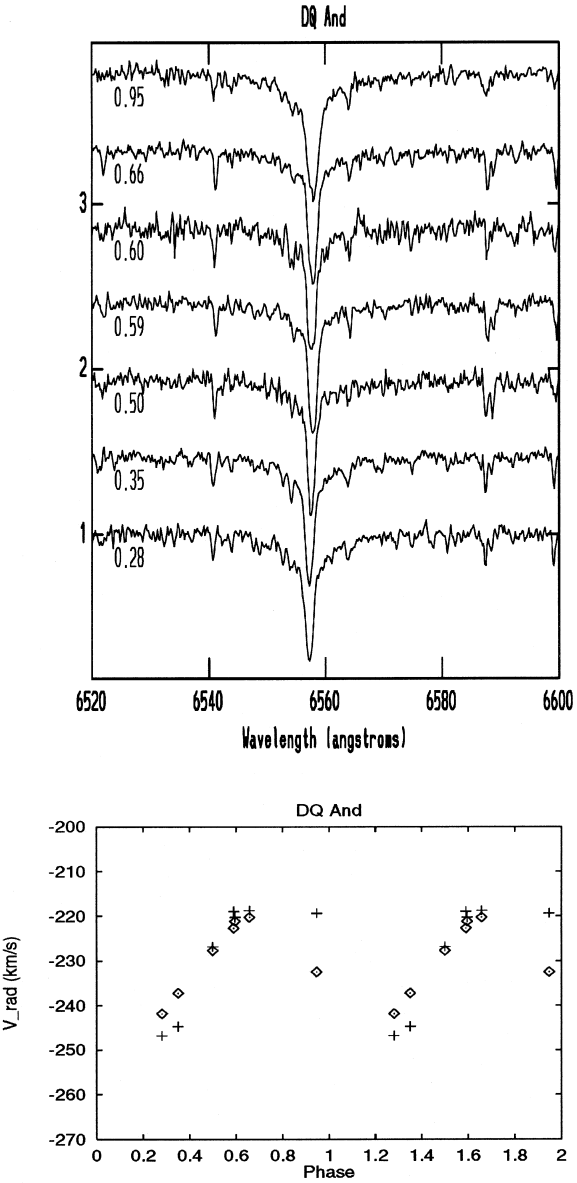

Figure 9. The same as Fig. 6 for DQ And.

1997) TX Del seems to have too large a radius for being a normal Type II Cepheid; it is therefore suspected that this star is a peculiar classical (massive supergiant) Cepheid far from the Galactic plane. The spectra of TX Del presented here (Fig. 14) do not contain any specific feature that can be used to classify TX Del as either a Population I or a Population II star – these spectra are similar to that of either classical Cepheids or other Population II stars in this paper.

BD Cas, V572 Aql, V383 Cyg

As found by Harris & Wallerstein (1984), these comparatively short-period Population II Cepheids do not show Hα emission.

DQ And, KL Aql, V733 Aql, BB Her

These stars are also 'suspected Type I' Cepheids from the sample of Balog et al. (1997). Again, as in the case of TX Del, there are no special features in their spectra that would indicate their belonging to Type II Cepheids.

None of the spectra of the stars with $P_{\rm pul}=3$–8 d show line doubling or emission features (as, e.g., BL Her does), which fully confirms the results of previous investigators (e.g. Harris & Wallerstein 1984). This means that either (i) the linear relation between the time-scale of the hydrogen emission and the pulsational period proposed by Kraft et al. (1959) is not valid in this period regime, or (ii) all these stars observed by us are actually Type I Cepheids (the relation of Kraft et al. is only for Type II Cepheids). The latter statement would confirm the results of Balog et al. (1997).

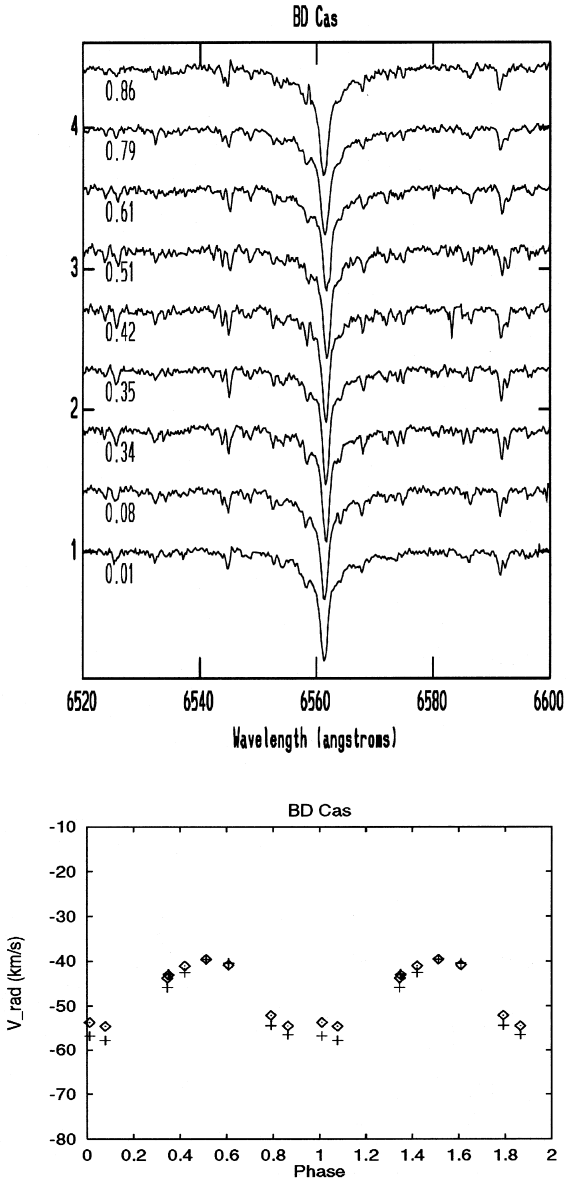

Figure 10. The same as Fig. 6 for BD Cas.

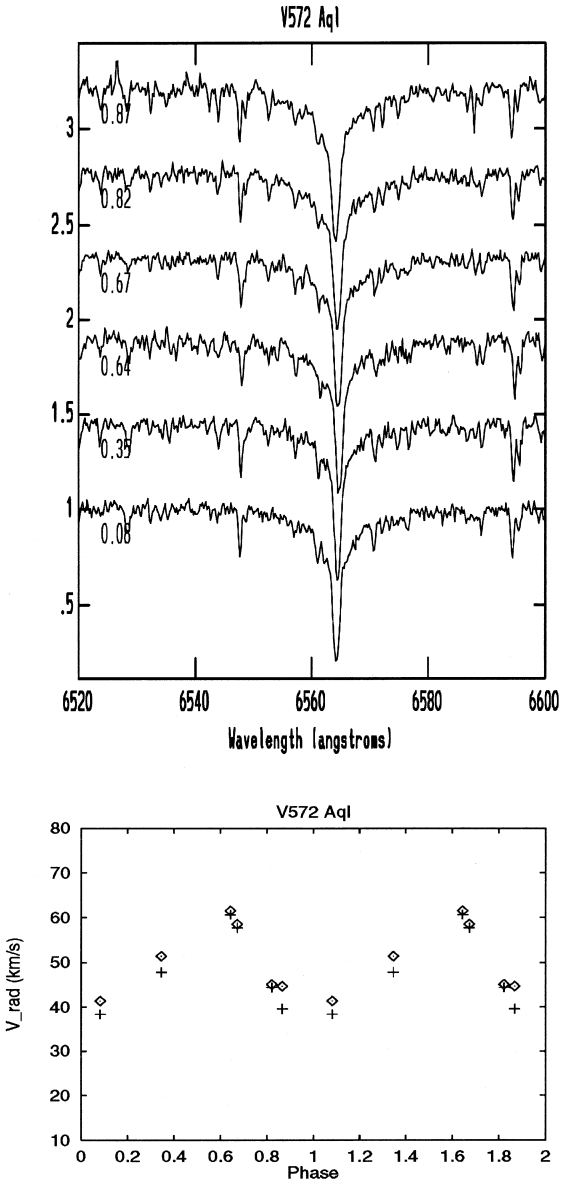

Figure 11. The same as Fig. 6 for V572 Aql.

AP Her

The period of this Cepheid is strongly variable (Szabados 1981), and therefore it is difficult to calculate the phases of the observations. Unfortunately, no additional photometry is available for the 1995 season, so the phases in Table 2 were computed with an approximate epoch and period: $T_0 = \text{JD } 2449902.0$ and $P = 10.4$ d. The Hα profiles of both AP Her and IX Cas are much more symmetric and less complicated than that of, e.g., κ Pav ($P_{\rm pul} \approx 9.08$ d) presented by Wallerstein et al. (1992). This indicates that the atmospheres of Type II Cepheids with $P_{\rm pul} = 9$–10 d can exhibit either strongly shocked or quite smooth pulsation.

The repetition of the spectra was also studied using those data that were observed on different nights when the star was in the same phase. The maximum allowed phase difference was set to 0.01. Spectra of four stars (V733 Aql, BB Her, IX Cas and AP Her) met this criterion (the phases can be found in Tables 2 and 3). The comparison of the spectra belonging to the same star and the same phase was made by computing the ratio of the spectra which enhance the small differences between the two data sets. When possible, the spectrum with higher S/N ratio was used in the denominator in order to reduce the scattering caused by the division. The only significant differences (i.e., those that exceed the noise level by at least 1σ) in this spectral region at the phases tested that were found for all stars were entirely due to the change of telluric line strengths from night to night. This indicates that (i) the repeatability of the measurements was comparable with the accuracy of the individual data, and (ii) the four Cepheids studied in this way did not show any cycle-to-cycle variation in the observed spectral regime at the phases tested.

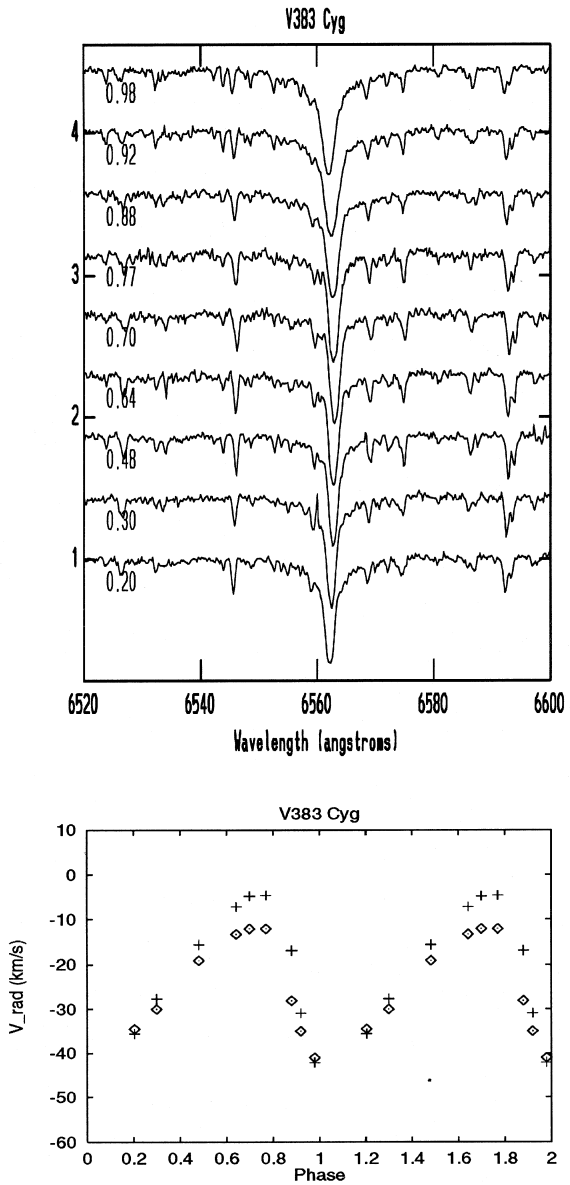

Figure 12. The same as Fig. 6 for V383 Cyg.

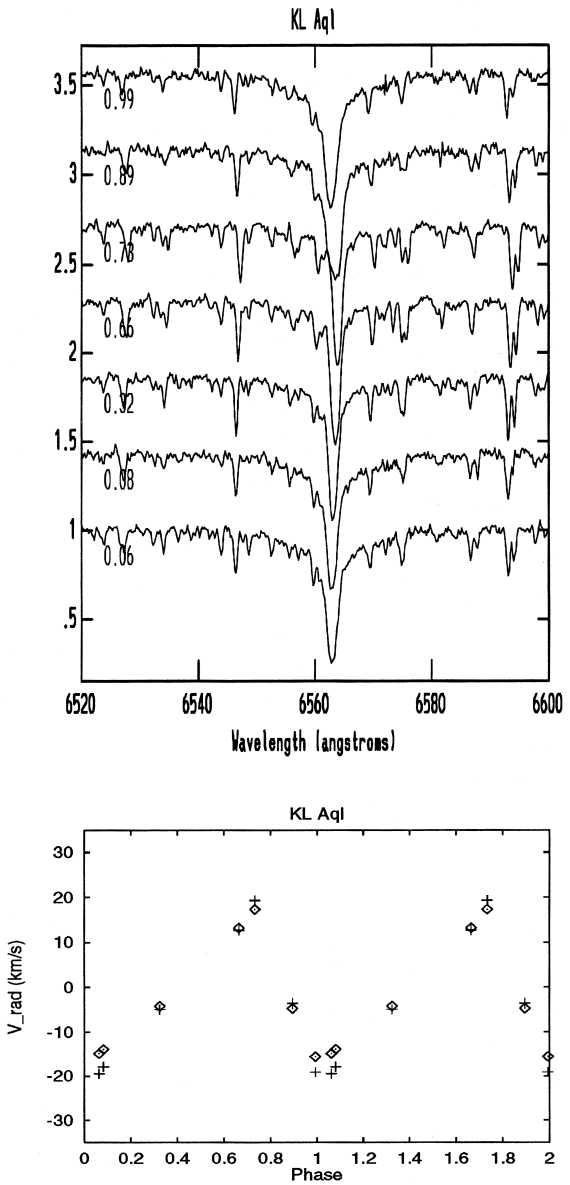

Figure 13. The same as Fig. 6 for KL Aql.

4 VELOCITY DIFFERENCES

In order to compare our results with those of previous investigations, Hα velocities of Cepheids were collected from the literature. The references are listed in Table 4. The general conclusion of the earlier results was that there are always velocity differences between the photospheric (metal) and upper atmospheric (hydrogen) velocities which are the strongest during the outward acceleration phases. However, the size of the velocity difference varies from star to star. Having a set of velocity information for Cepheids with various physical parameters, the question may arise – can we find any correlation between the velocity differences and the physical state of the atmosphere? Such a correlation would enable us to compare the model computations with observations.

In order to study this problem empirically, a simple parameter was introduced: the maximum amount of velocity difference between metallic and Hα velocities (see Table 4). The formation of the Hα line in a non-stationary atmosphere is complicated and probably takes place over many different atmospheric layers (see, e.g., Fokin & Gillet 1994 and Albrow & Cottrell 1996). The difference between these two measured velocities cannot be related simply to velocities at different levels. However, the measured difference is determined by the velocity differences throughout the atmosphere. Basically, the maximum velocity difference depends on two quantities: (1) the velocity difference between the photosphere and the upper atmosphere from which Hα emerges, and (2) the phase difference between the motion of these two regions.

Since the Hα velocities depend sensitively on the method of assigning Doppler shift to a strong, sometimes asymmetric line (see Section 2), it is necessary to measure these velocities in a homogeneous way. The 0.9 bisector velocities were therefore adopted for this purpose, because these

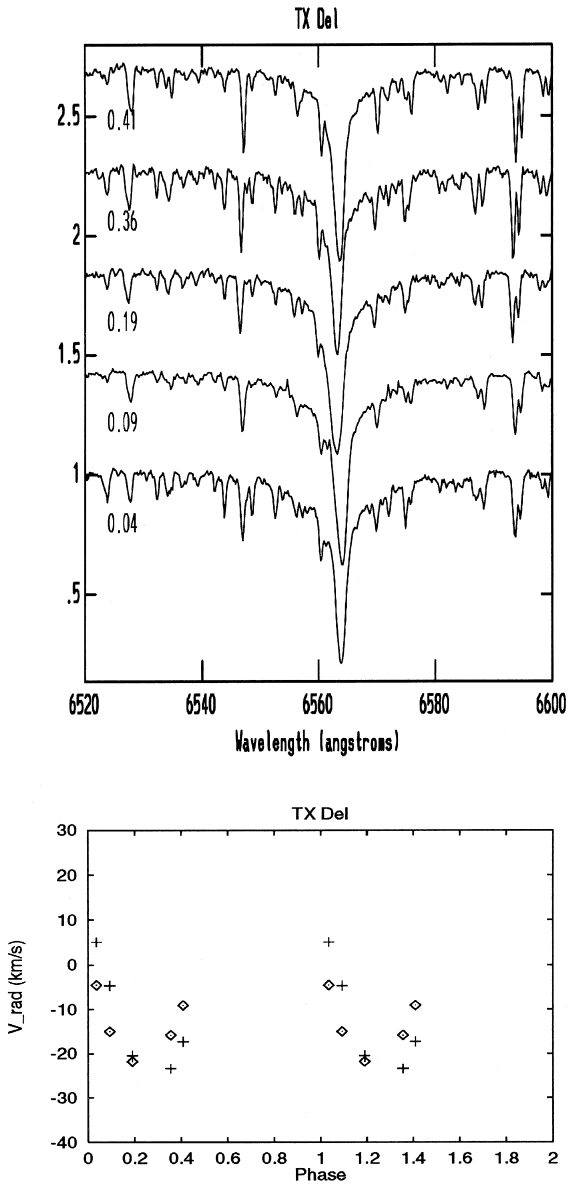

Figure 14. The same as Fig. 6 for TX Del. The velocities have been corrected for orbital motion.

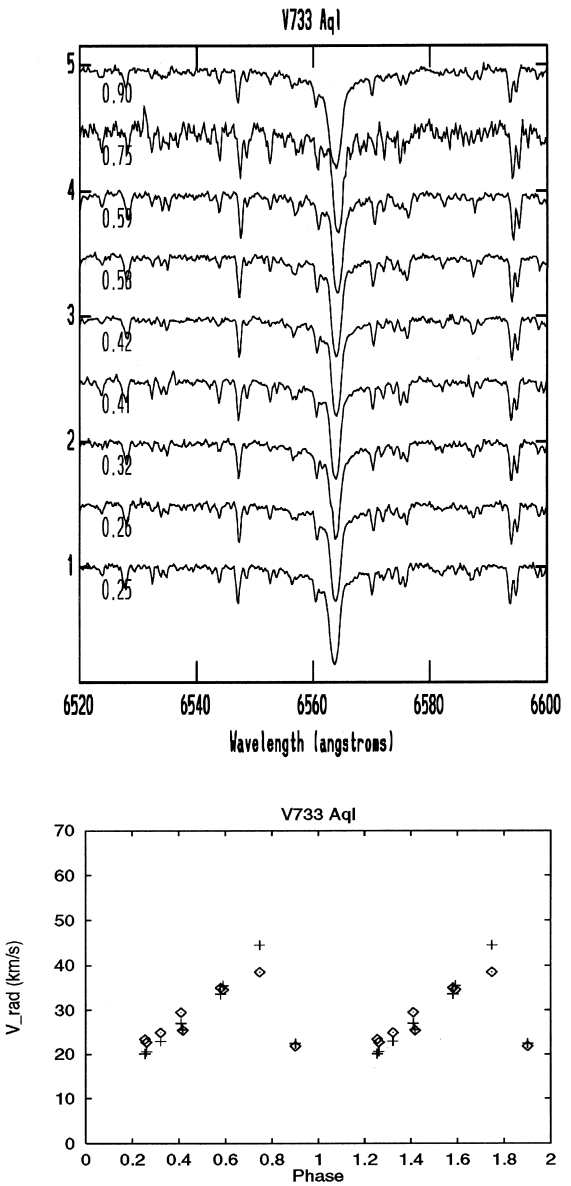

Figure 15. The same as Fig. 6 for V733 Aql.

were usually given by previous investigators (see Wallerstein et al. 1992). As was mentioned in Section 2, the metallic-line velocities measured by the 0.9 bisector and cross-correlation methods usually agree within the accuracy of our velocity determination ($\sim$1 km s^{-1}). Thus the results presented in this section are valid for the 0.9 bisector velocities of Hα. At present, the use of other bisector levels or other kinds of velocities is restricted by the small amount of available data. Table 4 lists the type of the Cepheid, the period, the velocity and light-curve amplitude, the maximum velocity difference computed with the 0.9 bisector and the reference for the Cepheids collected from the available literature and from this paper.

In Fig. 19 the maximum velocity difference is plotted against period. Classical (Type I) Cepheids are indicated as diamonds, while Type II Cepheids are shown as plus signs. The stars with uncertain maximum velocity differences are also plotted as squares. For these stars the phase coverage is not enough to derive the maximum of the velocity differences, so this parameter is underestimated (marked with a colon in Table 4) in these cases. As a result, the data marked with square symbols represent only the lower limit of the maximum velocity difference.

Fig. 19 shows that the maximum velocity difference depends strongly on period. There is a general trend that the longer the period, the larger the maximum velocity difference. However, this is not true for the very short-period star BL Her. At $P = 10$ d the velocity difference function sharply increases and seems to show a saturation effect at $P > 20$ d, although this is uncertain since it is based on only a few stars. In the long-period regime the only exception is Y Oph, which has unusually low velocity amplitude (Wallerstein et al. 1992).

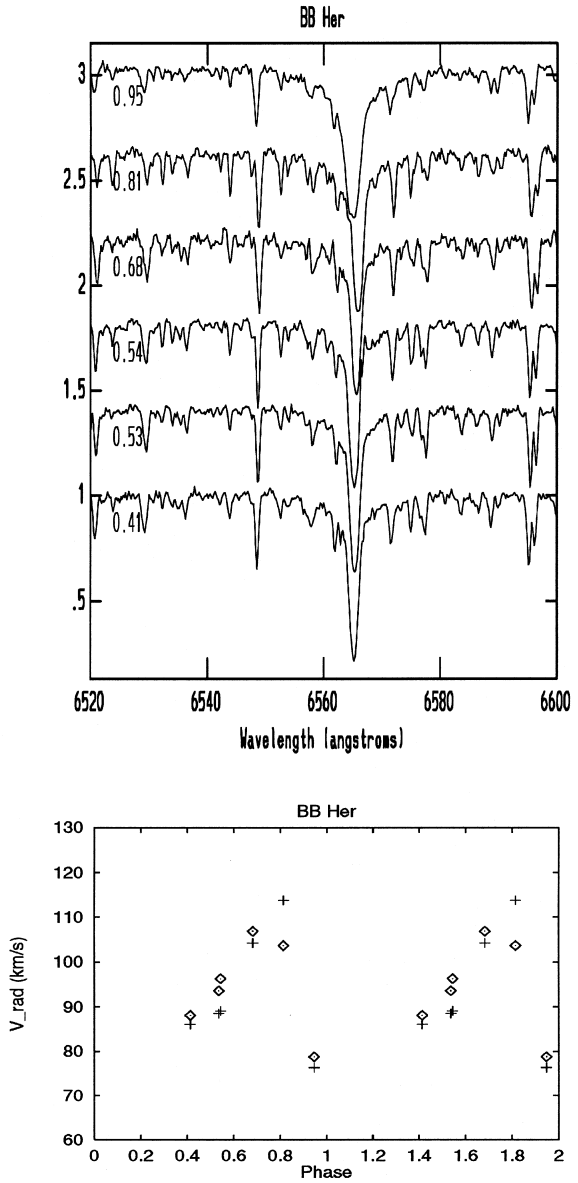

Figure 16. The same as Fig. 6 for BB Her.

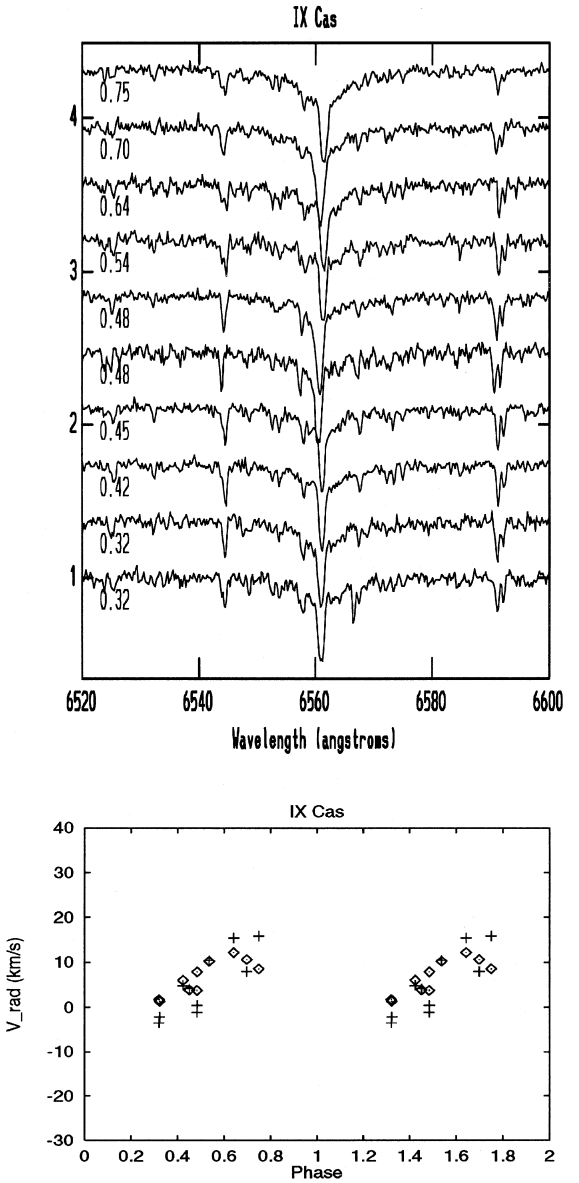

Figure 17. The same as Fig. 6 for IX Cas. The velocities were corrected for orbital motion.

It is expected that the velocity differences should depend on the velocity amplitude of the photosphere, since stronger pulsation should produce larger velocities in the outer regions. Fig. 20 shows the dependence of the velocity differences on the velocity amplitude. The maximum velocity difference increases with increasing amplitude. This is consistent with the prediction of pulsation theory, because the photosphere where most of the metallic lines are formed, and the outer layers from which Hα emerges, can be considered as coupled oscillators. If the velocity of the photospheric motion grows, it excites larger scale oscillations in the outer zones, and so the velocity difference increases.

In Fig. 20 the largest scattering occurs in the 20–40 km s^{-1} amplitude interval where the velocity difference varies considerably from star to star between 3 and 45 km s^{-1}. It is interesting that within the 30–40 km s^{-1} amplitude interval most of the Cepheids with small maximum velocity difference belong to Type II, while the ones with large velocity differences are of Type I. Since this is based on a few stars, it may be a selection effect; however, a hypothesis that it reflects real physical differences cannot be ruled out. This latter suspicion can be strengthened by the similar behaviour found in Fig. 21, where the maximum velocity differences are plotted by the similar behaviour found in Fig. 21, where the maximum velocity differences are plotted against the *V* light-curve amplitude. The general trend is similar to that in Figs 19 and 20, and the largest variation of the maximum velocity difference from star to star can be seen in the 0.5–0.8 mag amplitude interval (in the middle of Fig. 21). The same separation of Type I and Type II Cepheids as that mentioned before can be observed. However, the similarity of Figs 19–21 can be explained by the existing relation between the pulsational period and either velocity

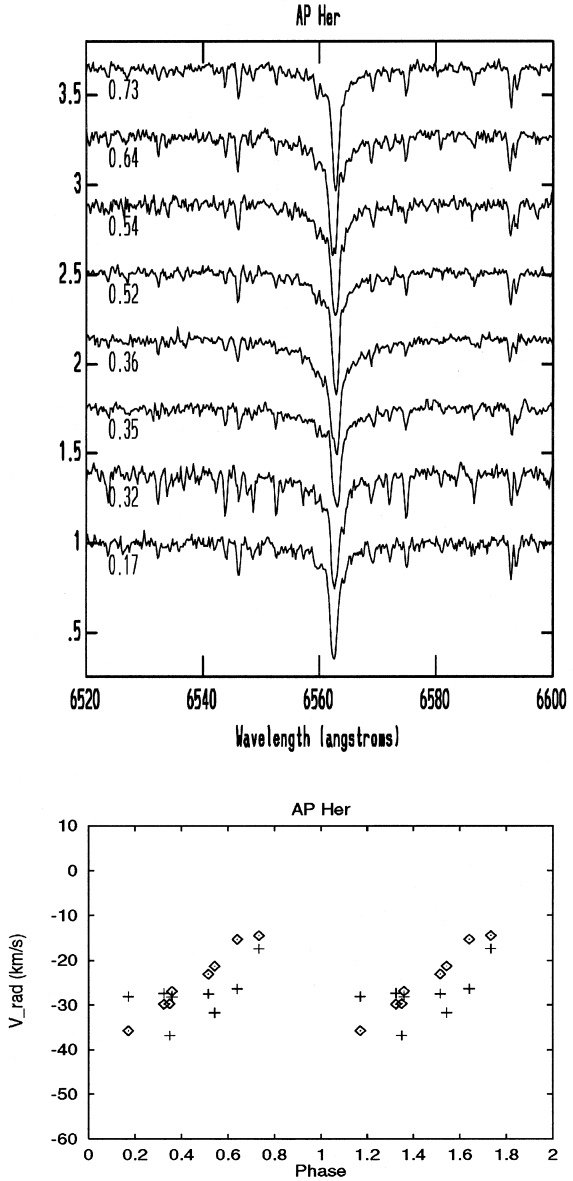

Figure 18. Hα line profiles and velocities of AP Her. The phases have been computed for an approximate epoch and period (see text).

Table 3. Orbital and pulsational velocities for binary Cepheids.

JD	ϕ_{pul}	V^{obs}_{met}	$V^{obs}_{H\alpha}$	V^{orb}	V^{pul}_{met}	$V^{pul}_{H\alpha}$
AU Peg	Template: HD187691 (F8V)					
49957.764	0.6244	−43.9	−72.8	−41.8	−2.1	−31.0
49959.776	0.4581	−51.9	−70.6	−39.4	−12.5	−31.2
49959.791	0.4631	−51.3	−69.7	−39.3	−11.9	−30.3
49961.787	0.2906	−51.9	−58.7	−35.1	−16.8	−23.6
49965.670	0.9022	14.4	−42.0	−22.1	7.7	−19.9
49976.772	0.5046	26.1	−3.6	34.1	−8.0	−37.7
49978.598	0.2612	23.0	2.8	41.7	−18.7	−38.9
49979.532	0.6480	43.6	10.9	44.9	−1.3	−34.0
49986.590	0.5746	44.1	17.6	48.5	−4.4	−30.9
49987.758	0.0589	47.0	24.5	45.3	1.7	−20.8
49988.747	0.4685	30.7	19.0	41.8	−11.1	−22.8
49989.722	0.8735	44.3	25.4	37.8	6.5	−12.4
49989.746	0.8831	43.0	24.1	37.7	5.3	−13.6
49990.544	0.2135	19.2	20.5	34.0	−14.8	−13.5
49990.740	0.2944	16.4	14.9	33.0	−16.6	−18.1
49991.731	0.7056	30.2	16.8	27.9	2.3	−11.1
50003.622	0.6356	40.9	−57.8	−33.5	−7.4	−24.3
50004.513	0.0050	−23.7	−46.3	−36.1	12.4	−10.2
50007.521	0.2521	−56.5	−61.7	−41.4	−15.1	−20.3
50009.545	0.0925	−42.5	−60.1	−42.3	−0.2	−17.8
TX Del	Template: HD23169 (G2V)					
49988.7180	0.0356	10.2	19.7	14.7	−4.5	5.0
49989.6703	0.1900	−6.5	−13.1	15.3	−21.8	−20.4
49990.6889	0.3552	0.1	−7.5	15.9	−15.8	−23.4
50007.5672	0.0926	9.5	19.8	24.5	−15.0	−4.7
50009.5156	0.4086	16.1	8.6	26.0	−9.1	−17.3
IX Cas	Template : HD23169 (G2V)					
49961.858	0.4836	−88.0	−92.9	−91.7	3.7	−1.2
49978.694	0.3227	−70.9	−74.4	−72.2	1.3	−2.2
49979.866	0.4508	−68.0	−67.7	−71.9	3.9	4.1
49987.825	0.3202	−71.4	−76.6	−73.1	1.7	−3.5
49988.772	0.4236	−67.7	−68.9	−73.7	6.0	4.8
49989.805	0.5364	−64.2	−64.0	−74.4	10.2	10.4
49990.770	0.6419	−63.0	−59.8	−75.2	12.2	15.4
49991.758	0.7498	−67.5	−60.2	−76.0	8.5	15.8
50007.838	0.4844	−89.7	−97.1	−97.6	7.9	0.5
50009.594	0.6981	−90.1	−92.8	−100.7	10.6	7.9

or light-curve ampliude (except the very short-period stars which do not obey the same relation as longer period ones).

A qualitative explanation of the sharp increase of the maximum velocity difference in the middle of Figs 19–21 is possible if we consider the phase differences between the motion of the photosphere and the 'Hα layer' which is well above the photospheric zone. The velocity difference is a function of the phase shift between two coupled oscillators, and its maximum depends sensitively on the actual value of the phase shift. Since the time needed for a running wave passing through the atmosphere to reach the upper atmospheric layers is roughly the geometric distance between the photosphere and the 'Hα layer' divided by the average sound speed, such a phase shift can be expected, and it may vary from star to star according to the varying radius, atmospheric parameters, etc. of the individual stars.

The structure of the data in Figs 19–21 might mean that there is a jump in the phase difference roughly at $\log P = 1.0$ or at $K = 30$–40 km s^{-1}. At shorter periods (for $3 < P < 10$ d) and lower amplitudes the photosphere and the 'Hα layer' move together during the whole pulsational cycle, while at longer periods or larger amplitudes these two layers can move in opposite directions at certain phases: the photosphere expands while the outer layers still fall inward. It is known that $\log P = 1.0$ is close to the centre of the 2:1 resonance between the fundamental mode and the second overtone in classical Cepheids, so such a phase jump between different layers might be reasonable. (As pointed out by the referee, BL Her is an exception to the trend in Fig. 19.)

The problem with this interpretation is that the term 'Hα layer' cannot be assigned to a single physical layer with a fixed column mass density during the whole cycle, as was shown in many papers (e.g. Grenfell & Wallerstein 1969; Wallerstein 1983). Thus the velocities derived from the Hα

Table 4. Velocity differences between metallic and hydrogen lines. The meaning of the symbols is as follows: P – period (in d), K – total amplitude of the velocity curve (in km s^{-1}), ΔV – total amplitude of the light curve (in mag), ΔVel. – maximum value of Hα minus metallic velocity (in km s^{-1}). In this column the colon marks represent uncertain (underestimated) values (see text). In the reference column the symbols mean the following: A – Wallerstein et al. (1992); B – Wallerstein (1979(; C – Lèbre & Gillet (1992); D – Raga et al. (1989); E – Grenfell & Wallerstein (1969); F – Kiss et al. (in preparation); p.p. – present paper.

Star	Type	P	K	ΔV	ΔVel.	ref.
BL Her	II	1.31	42	0.85	54	p.p.
SW Tau	II	1.58	35	0.74	9:	p.p.
SU Cas	I	1.95	18	0.41	3:	F
DT Cyg	I	2.50	13	0.29	4	F
SZ Tau	I	3.15	15	0.33	10	F
DQ And	II?	3.20	35	0.75	24:	p.p.
HD32456	I	3.29	27	0.60	9:	F
V1334 Cyg	I	3.33	10	0.15	5:	F
BD Cas	II	3.65	18	0.32	2	p.p.
RT Aur	I	3.73	35	0.80	9:	F
V572 Aql	II	3.77	23	0.41	3	p.p.
T Vul	I	4.43	30	0.64	15:	F
V383 Cyg	II	4.61	30	0.54	14	p.p.
δ Cep	I	5.37	38	0.83	10	B
KL Aql	II?	6.11	36	0.76	13	p.p.
TX Del	II?	6.17	30	0.63	10:	p.p.
V733 Aql	II?	6.18	24	0.45	11	p.p.
η Aql	I	7.18	39	0.80	45	A
BB Her	II?	7.51	32	0.65	17	p.p.
W Sgr	I	7.60	39	0.81	40	A
S Sge	I	8.38	37	0.72	31	F
κ Pav	II	9.08	25	0.81	40	A
IX Cas	II	9.15	20	0.52	7:	p.p.
S Mus	I	9.66	31	0.54	25	A
S Nor	I	9.75	34	0.65	30	A
β Dor	I	9.84	33	0.65	35	A
ζ Gem	I	10.15	27	0.48	38	A
AP Her	II	10.4	25	0.72	20:	p.p.
X Cyg	I	16.39	55	1.0	70	A
Y Oph	I?	17.12	17	0.49	4.5	A
W Vir	II	17.27	55	1.2	50	C, D
T Mon	I	27.02	47	1.02	60	A
U Car	I	38.77	47	1.19	60	A
SV Vul	I	45.00	44	1.06	60	E

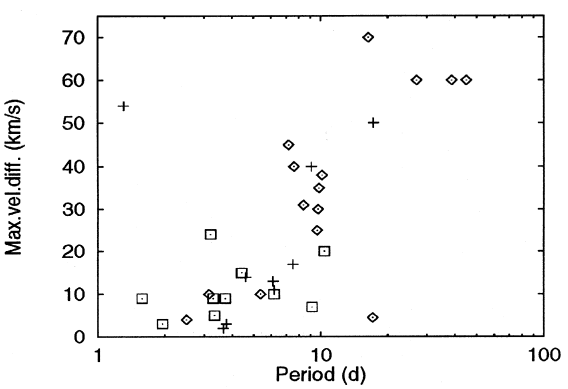

Figure 19. Maximum velocity difference against pulsational period. The symbols mean the following: diamonds – Type I Cepheids; plus signs – Type II Cepheids; squares – Cepheids of either type, but with underestimated maximum velocity difference.

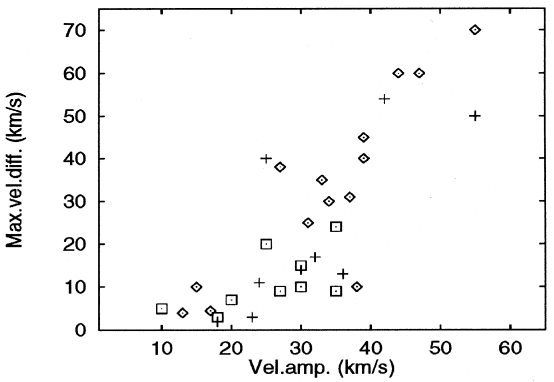

Figure 20. Maximal velocity difference against velocity amplitude.

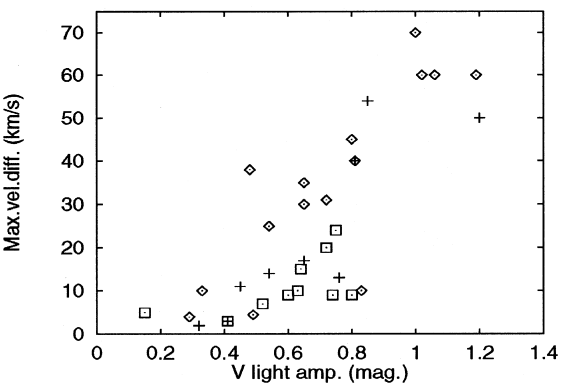

Figure 21. Maximum velocity difference against V light-curve amplitude.

line cannot be used in a simple kinematic model. Therefore the velocity differences should also be affected by the velocity gradients in the pulsating atmospheres (Albrow & Cottrell 1996). This means that there may be a selection mechanism that determines the amount of velocity gradient for a particular Cepheid. Physically this process might be connected with the shock propagation in the atmosphere. However, much more observational as well as theoretical data would be needed to understand these phenomena better and to draw a clearer picture of these processes.

If the diagrams in Figs 19–21 really represent the strength of velocity gradients in the stellar atmospheres, then long-period Cepheids would become less useful for direct calibration of period–radius and period–luminosity relations via Baade–Wesselink methods, because these stars usually have larger velocity differences; thus their velocity curves should depend largely on the spectral lines used for measuring Doppler shifts. This was recently pointed out by Sasselov & Lester (1990) and Butler, Bell & Hindsley (1996). They found 15–20 per cent error in the derived radius due to the effect of velocity gradients. Their programme stars are all in the high-difference regime, which may confirm that Hα and metallic lines can be used to estimate the amount of velocity gradients. Thus it is especially important to select specific lines with known formation depth in order to get reliable velocity curves of long-period Cepheids.

The increasing amount of high-resolution spectroscopic data will hopefully enable us to get a better picture of pulsating atmospheres in the future. This would be very important for deriving more reliable fundamental parameters of these stars. From the observations presented in this paper it seems that the atmosphere of intermediate-period Cepheids behaves less extremely than that of most long- and short-period Cepheids. Further observations including spectroscopic study of fainter stars of both types are planned to extend the empirical knowledge of Cepheid atmospheres.

5 SUMMARY

Based on the results presented in the previous sections we draw the following conclusions.

(1) In accordance with earlier studies we have found that there is no hydrogen emission in the spectra of intermediate-period Type II Cepheids. These stars behave similarly to their Type I counterparts, which also do not show any hydrogen emission.

(2) Unlike any other Cepheids in our programme, the Hα line profile of AU Peg shows a P Cygni-like feature. This might be due to a mass outflow from the system, which may be connected with the dust shell shown by the *IRAS* measurements.

(3) The Hα profiles of the Type II Cepheids IX Cas ($P=9.15$ d) and AP Her ($P=10.4$ d) are much more symmetric and less disturbed than those of κ Pav ($P=9.08$ d) and some other classical Cepheids which have similar periods. This indicates that the atmospheric pulsation characteristics of Cepheids in this period regime can vary considerably from star to star. On the other hand, no significant cycle-to-cycle variations of the spectral features of the programme stars could be detected.

(4) The comparison of Hα radial velocities obtained from cross-correlation and bisector techniques shows that the largest differences occur during the outward acceleration phases when the line asymmetries are expected to be the greatest. This is in agreement with the results of Wallerstein et al. (1992) for classical Cepheids.

(5) The maximum velocity differences between metallic and Hα lines are smaller for most of the stars studied here (except for BL Her) than for longer period Cepheids. This may mean that the pulsating motion of these atmospheres is less complicated, and so these stars should be more suitable targets for calibration purposes.

ACKNOWLEDGMENTS

JV and LLK acknowledge the warm hospitality of York University, David Dunlap Observatory and University of Toronto where the major part of this work has been done. We thank the staff of David Dunlap Observatory for kindly granting the necessary telescope time. Special thanks are due to Jim Thomson and Steve Smith for their keen assistance during the observing run. This research was supported by Hungarian OTKA Grants F022249, W015239, T14852, T022946 and the Hungarian Eötvös Fellowship to JV. Financial support was also provided from the *AXAF* Science Center NASA contract NAS8-39073. The SIMBAD data base and the ADS Abstract Service was used to access data and references, and these are also gratefully acknowledged.

REFERENCES

Abt H. A., 1954, ApJS, 1, 63
Albrow M. D., Cottrell P. L., 1996, MNRAS, 278, 337
Baird S. A., 1982, PASP, 94, 850
Balog Z., Vinkó J., Kaszás G., 1997, AJ, 113, 1833
Breitfellner M. G., Gillet D., 1993, A&A, 277, 553
Butler R. P., 1993, ApJ, 415, 323
Butler R. P., Bell R. A., Hindsley R. B., 1996, ApJ, 461, 362
Evans N. R., 1991, ApJ, 372, 597
Evans N. R., 1992, ApJ, 389, 657
Evans N. R., Lyons R., 1986, AJ, 92, 436
Fokin A. B., Gillet D., 1994, A&A, 290, 875
Gillet D., Burki G., Chatel A., Duquennoy A., Lèbre A., 1994, A&A, 286, 508
Gingold R. A., 1985, Mem. Soc. Astron. Ital., 56, 169
Gorynya N. A., Samus N. N., Rastorguev A. S., Sachkov M. E., 1996, Pis'ma Astron. Zh., 22, 198
Grenfell T. C., Wallerstein G., 1969, PASP, 81, 732
Harris H. C., Wallerstein G., 1984, AJ, 89, 379
Harris H. C., Welch D. L., 1989, AJ, 98, 981
Harris H. C., Olszewski E. W., Wallerstein G., 1984, AJ, 89, 119
Hinkle K. H., Hall D. N. B., Ridgway S. T., 1982, ApJ, 252, 697
Joy A. H., 1949, ApJ, 110, 105
Kraft R. P., Camp D. C., Hughes W. T., 1959, ApJ, 130, 90
Laney C. D., 1995, in Stobie R. S., Whitelock P. A., eds, ASP Conf. Ser. Vol. 83, Proc. IAU Colloq. 155, Astrophysical Application of Stellar Pulsation. Astron. Soc. Pac., San Francisco, p. 367
Lèbre A., Gillet D., 1992, A&A, 255, 221
McAlary C. W., Welch D. L., 1986, AJ, 91, 1209
Pollard K. R., Cottrell P. L., Lawson W. A., Albrow M. D., Tobin W., 1997, MNRAS, 286, 1
Raga A., Wallerstein G., Oke J. B., 1989, ApJ, 347, 1107
Sabbey C. N., Sasselov D. D., Fieldus M. S., Lester J. B., Venn K. A., Butler R. P., 1995, ApJ, 446, 250
Sanford R. F., 1952, ApJ, 116, 331
Sasselov D. D., Lester J. B., 1990, ApJ, 362, 333
Schwarzschild M., 1952, Trans. IAU, 8, 811
Szabados L., 1981, Commun. Konkoly Obs. Budapest No. 77
Vinkó J., Szabados L., Szatmáry K., 1993, A&A, 279, 410
Wallerstein G., 1958, ApJ, 127, 583
Wallerstein G., 1979, PASP, 91, 772
Wallerstein G., 1983, PASP, 95, 422
Wallerstein G., Cox A. N., 1984, PASP, 96, 677
Wallerstein G., Elgar S., 1992, Sci, 256, 1531
Wallerstein G., Jacobsen T. S., Cottrell P. L., Clark M., Albrow M., 1992, MNRAS, 259, 474